Pure Appl. Chem., Vol. 83, No. 2, pp. 325–343, 2011.
doi:10.1351/PAC-CON-10-07-08

Zeolite-modified electrodes with analytical applications*

Liana Maria Muresan

Department of Physical Chemistry, Babeş-Bolyai University, 11 Arany J. Street, 400028 Cluj-Napoca, Romania

Abstract: Zeolite-modified electrodes (ZMEs) have been widely investigated because of their chemical, physical, and structural characteristics (shape, size, and charge selectivities; physical and chemical stabilities; high ion-exchange capacity; hydrophilic character; etc.), which make them of high interest in the design of electroanalytical systems. The paper presents recent literature data about fundamental and practical aspects related to the obtaining and applications of ZMEs. Some new ZMEs based on carbon paste incorporating soluble phenothiazinic dyes adsorbed on X-type zeolites are assessed comparatively, and the influence of some experimental parameters on the electrochemical response of these electrodes was investigated. The kinetic parameters for the heterogeneous electron-transfer process corresponding to the surface-immobilized mediators were determined, and all observed differences were used as evidence of the influence of the mediator structure and of the zeolite nature on the electrochemical activity of the new electrodes and on their electrocatalytic properties toward β-nicotinamide adenine dinucleotide (NADH) or ascorbic acid (AA) electro-oxidation and H_2O_2 electroreduction.

Keywords: amperometric detection; ascorbic acid; H_2O_2; methylene blue; β-nicotinamide adenine dinucleotide (NADH); phenothiazinic dyes; zeolites; zeolite-modified electrodes.

ZEOLITES: STRUCTURE AND PROPERTIES

Zeolites are crystalline, microporous, aluminosilicate materials with well-defined structures. Generally, they contain silicon, aluminum, and oxygen in their framework and cations, water, and/or other molecules within their pores. Zeolites have the capacity to be completely hydrated and dehydrated without damage to the crystalline lattice [1].

A general formula of aluminosilicate zeolites is: $M_aD_bT_c[Al_{(a+2b+3c)}Si_{[x-a+2b+3c)]}O_{2x}]\cdot mH_2O$, where M, D, T are mono-, di-, and trivalent extra-framework cations which maintain the electrical neutrality [2].

Many zeolites occur naturally as minerals, and are extensively mined in many parts of the world. Others are synthetic, and are made commercially for specific uses, or produced by research scientists trying to understand more about their chemistry.

Natural zeolites form where volcanic rocks and ash layers react with alkaline groundwater. Their structure has more acid-resistant silica to hold the structure together; they are rarely pure and are contaminated to varying degrees by other minerals, metals, quartz, or other zeolites. For this reason, natu-

*Paper based on a presentation made at the 2nd Regional Symposium on Electrochemistry: South East Europe (RSE SEE-2), Belgrade, Serbia, 6–10 June 2010. Other presentations are published in this issue, pp. 253–358.

rally occurring zeolites are excluded from many important commercial applications where uniformity and purity are essential. Moreover, although some natural zeolites occur in large amounts, they offer only a limited range of atomic structures and properties.

Synthetic zeolites are created through a slow crystallization process using a combination of silica and alumina and using a foundation of alkali and organic templates. They can be manufactured to provide a wide range of desired structures, adsorption characteristics, or selectivity, and can be used as a separation tool for numerous commercial applications.

Structural frameworks of zeolites, whether they are naturally occurring or synthetically designed, are documented and coded [3]. The primary building blocks of zeolites are SiO_4^{4-} and AlO_4^{5-} tetrahedra. These can link in several ways, resulting in distinct three-dimensional structures. In all, over 150 different framework structures are now known. The framework structure may contain linked cages, cavities, or channels that give rise to the molecular discriminatory nature of zeolites, which allows small molecules of the right size to enter. Between 20 and 50 % of the volume of zeolite is void.

The Si/Al ratios determine the acidity and hydrophilicity/-phobicity of zeolites [4]. A high content of aluminum in the zeolite structure leads to an increase of zeolite hydrophilicity. On the other side, the presence of Al in the framework induces a negative charge that is balanced by an extra-framework cation. This is exchangeable with other ions, offering a convenient method for implanting a variety of electroactive cations into zeolite micropores.

The key feature of zeolites is their microporosity. The pores can be one-, two-, or three-dimensional and span a range of shapes and sizes, roughly between 3 and 10 Å in diameter. Depending on the pores dimension and on the framework structure, zeolites can be A, X, Y, or L type (Fig. 1).

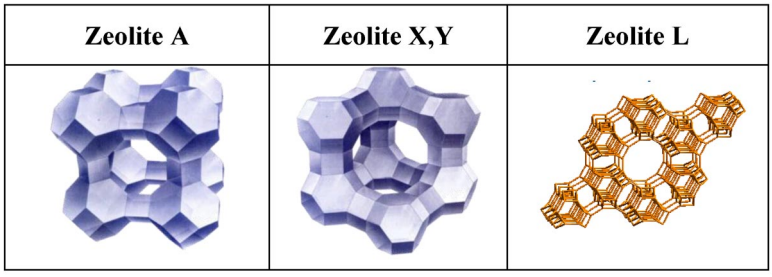

Fig. 1 Zeolite types.

Zeolite A is a small-pore zeolite in which the Si/Al ratio is equal to 1, and the cages are linked octahedrically. The zeolite A synthesis produces precisely duplicated sodalite units which have 47 % open space, ion-exchangeable sodium, water of hydration, and electronically charged pores. Depending on the nature of the extra-framework cation, the pore diameter varies from about 3 to 5 Å. Zeolites X and Y are large-pore zeolites (6–8 Å) containing various Si/Al ratios and tetrahedrically linked cages. Zeolites L contain flat cylindrical crystals, of "hockeypuck" or "coin" shape assembled in hexagonal systems and linear channels in which one-dimensional diffusion takes place.

All aluminosilicate zeolites offer a number of chemical, physical, and structural characteristics of high interest in the design of electroanalytical systems: shape, size, and charge selectivities; physical and chemical stabilities; high ion-exchange capacity; and hydrophilic character [5–7].

Due to their rigid, three-dimensional, and negatively charged lattice, zeolites act as molecular sieves, offering molecular discrimination/recognition [2]. Under equilibrium conditions, only non-size-excluded species can enter and are able to diffuse freely into the zeolite framework. This property can be exploited to promote the selective preconcentration of analytes at electrochemical surfaces and to confine redox mediators in the cavities of zeolites.

An important intrinsic property of most zeolites is their ability to undergo ion exchange. The most common use of ion exchange is for water-softening and demineralization of water [8]. Ion exchange can also be used as an alternative method for treatment of industrial wastewaters such as metal-finishing effluents [9,10], by precipitation methods. The combination of the cation-exchange capacity of the aluminosilicate zeolites and the molecular sieving ability is used to create intelligent electrode materials for electroanalytical purposes.

Protonated zeolites have acidic properties. The protons that balance the negative charge of a zeolite framework are not strongly bound to the framework and are able to move within the pores and react with molecules which penetrate into the zeolite pore system. A protonated zeolite thus can act as a Brønsted acid. Furthermore, Lewis acidity can be caused by cations within the pores.

Other advantageous features of zeolite modifiers are durability, dimensional stability, and, last but not least, their catalytic properties [1].

This is why involving zeolites in electrochemistry represents a challenge and an attractive goal. The intersection of electrochemistry and zeolite science results in a variety of interesting applications ranging from electrocatalysis [11] to analytical determinations [2].

ZEOLITE-MODIFIED ELECTRODES

As already mentioned, zeolites offer a number of characteristics (molecular sieve selectivity, cation-exchange capacity, catalytic properties, etc.) of real interest in the design of electrochemical sensors. Moreover, the three-dimensional zeolite lattice offers a cage-and-channel architecture of molecular size, which can be exploited for entrapment of various redox mediators and enzymes in order to obtain electrochemical biosensors.

Zeolite-modified electrodes (ZMEs) form a subcategory of the chemically modified electrodes, which are the results of an intelligent design of the surface of conventional electrodes in order to improve their response, by combining the intrinsic properties of a modifier to a selected electrochemical reaction [5]. ZMEs became popular in the mid-1980s, and in recent decades, numerous studies have been devoted to understanding their properties. Their main advantage consists of combining in a single device the specificity of charge-transfer reactions with the molecular sieving and ion-exchange properties of the aluminosilicates. On the other hand, the hydrophilic character of zeolites makes them materials suited for the co-immobilization of enzymes and mediators in the preparation of biosensors [12]. Any electrochemical scheme that relies on ion exchange, analyte preconcentration, size/shape/charge selectivity, or any combination of these features can be designed for use in ZMEs.

Preparation methods

Efforts have been made to prepare reproducible ZMEs with desired properties. Some of the methods reported in the literature for the preparation of ZMEs are summarized in Table 1.

In the majority of cases, a conducting component (usually, graphite) was used for obtaining ZMEs, whereas the binders used included epoxy resins, petroleum jelly, mineral oil, or paraffin oil. Although many different methods were applied to the confinement of zeolites at an electrode surface, the main problem of ZMEs, particularly for electroanalysis, as stated by Walcarius [5] is the lack of reproducibility, due to the hetereogeneous nature of most ZMEs. This is why the ideal preparation method is yet to be discovered for getting highly durable ZMEs displaying good sensitivity, high selectivity, and ensuring fully reproducible measurements.

Table 1 Main preparation methods of ZMEs.

No. crt.	Method	Examples	References
1	Dispersion of zeolite particles within solid matrices	Incorporation in carbon paste	[13–20]
		Incorporation in carbon–polymer composites	[21,22]
		Carbon–zeolite mixtures	[23,24]
2	Deposition of zeolites on conductive substrates	Deposition on ITO glass	[25]
		Spin coating	[26]
		Compression of zeolites on supports	[27]
3	Coating of zeolite on solid electrodes using polymers	Electrogenerated coatings	[28]
		Inclusion of conductive polymers in zeolites	[29–32]
		Adsorption of polymer on zeolites	[33–34]
		Evaporation of solvent from a polymer–zeolite dispersion	[35]
		Thermic polymerization	[36]
4	Covalent binding of zeolite particles to a conductive surface	Covalent linking of zeolite to an electrode surface via silane and siloxane bondings	[37]
5	Electrophoretic deposition onto electrode surfaces	Electrophoretic deposition on Pt RDE	[38]
		Electrophoretic deposition on stainless steel grid	[39]

Mechanism of charge transfer occurring at ZMEs

The application of electrochemistry on zeolite-containing systems has generated a large debate on the electron-transfer mechanisms associated with ZMEs.

In the general case, three basic models (extrazeolitic, intrazeolitic, and surface-mediated) have been proposed [5,35,39]:

In the *intrazeolitic* mechanism, the electroactive species E^{m+} is reduced inside the zeolite structure, while solution-phase electrolyte cations C^+ enter the framework in order to maintain the charge balance:

$$E_Z^{m+} = ne^- + nC_S^+ \Leftrightarrow E_Z^{(m-n)+} + nC_Z^+$$

In the *extrazeolitic* mechanism, the electron-transfer process takes place outside of the zeolite, being preceded by the ion exchange of the electroactive species with electrolyte cations:

$$E_Z^{m+} + mC_S^+ \Leftrightarrow E_Z^{m+} + mC_Z^+$$

$$E_S^{m+} + ne^- \Leftrightarrow E_Z^{(m-n)+}$$

In the *combined* mechanism, the electroactive species of the zeolite surface undergo initial electron transfer and subsequently experience outer-sphere electron-transfer processes with intrazeolite species. Each step requires charge compensation by the electrolyte cations.

$$E_{Z,surf}^{m+} + ne^- + nC_S^+ \Leftrightarrow E_{Z,surf}^{(m-n)+} + nC_{Z,surf}^+$$

$$E_{Z,surf}^{(m-n)+} + nC_{Z,surf}^+ + E_{Z,bulk}^{m+} \Leftrightarrow E_{Z,bulk}^{(m-n)+} + nC_{Z,bulk}^+ + E_{Z,surf}^{m+}$$

Analytical applications of ZMEs

The joined size selectivity and ion-exchange capacity of zeolite molecular sieves, largely exploited in catalysis, make them also attractive for analytical applications. In particular, they were successfully involved in electroanalysis, by combining these properties to the electrochemical detection.

Analytical applications of ZMEs are multiple and widespread. Depending on the role played by the zeolite, these applications are based on the following detection principles:

- The zeolite extracts and concentrates different species (mainly, metallic cations) from the adjacent solution, and these species are subsequently detected electrochemically, due to their electroactivity.
- The zeolite hosts a redox couple that plays the role of mediator, intermediating the detection of some chemical species from the solution.
- The zeolite plays the role of molecular sieve (an electroactive species hosted inside the zeolite, which can be detected outside of the zeolite, is replaced by neutral non-size-excluded molecules, which can be determined indirectly).

Consequently, the analytical applications of ZMEs could be classified into five main categories [5]:

- direct amperometric detection
- voltammetric detection after accumulation at open circuit
- indirect amperometric detection of non-electroactive species
- amperometric biosensors
- potentiometry using zeolitic membranes

Direct amperometric detection

A first example of direct detection using ZMEs is presented by Creasy and Shaw [40], who have exploited the preconcentration of methylviologen at a carbon paste electrode (CPE) modified with A and Y zeolites for the mediated electroreduction of dissolved oxygen. It was the first work demonstrating the ability of zeolites to support electrocatalysts useful in amperometric detection. This work was followed by many others, reporting immobilization of various compounds on zeolites, for the detection of different analytes such as hydrazine, β-nicotinamide adenine dinucleotide (NADH) etc., some of them being presented in Table 2.

Table 2 Examples of direct amperometric detection at ZMEs.

Analyte	Zeolite	Method	References
O_2	NaA and NaY + MV^{2+}	Deposition onto Pt	[41]
Hydrazine	NaY + Cu porphyrin	CPE	[42]
O_2	Zeolite L + poly(phenosafranine)	Deposition onto BPG	[43]
NADH	NaY (LZY-52) + YFc	CPE	[44]
Uric acid	Graphite–ZME doped with Fe(III)	Deposition on GC	[45]
Phenol	LZ Y52 (NaY), HNaY, NaX, NaA	Zeolite–graphite pellets	[46]
p-Cresol	Synthetic zeolites (MFI and FAU)	CPE	[47]
Ascorbic acid	Cu(II)-doped zeolite	Deposition onto Pt	[48]
H_2O_2	Fe-enriched natural zeolitic volcanic tuff	CPE	[49]

BPG = basal pyrolitic graphite; GC = glassy carbon

Voltammetric detection after accumulation at open circuit

The good affinity of zeolites for metallic ions was exploited for preconcentration followed by voltammetric measurements based on ZMEs. Due to their exemplary preconcentration effects, zeolites used for the preparation of sensing electrode can be expected to lead to better detection sensitivity. The ion-exchange properties were found to improve the voltammetric detection, and the reversibility of the process allowed a chemical regeneration of the electrodic surface. Metallic ions, but also dopamine, nitrophenol, atenolol etc., could be detected by using this method (Table 3). The most efficient determinations were obtained with the large-pore zeolites X and Y.

Table 3 Voltammetric determinations after preconcentration at ZMEs.

Analyte	Zeolite	Method	References
MV^{2+}, Cu^{2+}, $Ru(NH_3)_6^{3+}$	Zeolite Y	Deposition on Pt and GC	[50]
Ag^+	Zeolite 4A	CPE	[51]
Dopamine	Y zeolite	CPE	[52]
4-Nitrophenol	Zeolite mixture	CPE	[53]
Pb^{2+}, Cd^{2+}	Zeolites 4A, 5A, 13X, and Y	Electrophoretic deposition on Pt	[38]
Cu(II), Cd(II), Zn(II)	Zeolites 3A, 4A, and 13X	CPE	[13,54]
Tryptophan, uric acid, and ascorbic acid	Fe(III)-doped zeolite	CPE	[55]
Atenolol	Mordenite	CPE	[56]

Indirect amperometric detection of non-electroactive species

Zeolites cannot normally accommodate cations larger than their pore size. This peculiarity was exploited by using ZMEs doped with electroactive species for indirect amperometric detection of species that cannot usually be detected by this way. Thus, when a ZME doped with an electroactive species E^+ is immersed in a solution containing non-size-excluded cations (e.g., NH_4^+), an amount of E^+ species will be liberated by ion exchange and could be detected amperometrically at the electrode surface. Alkali, but also Ca^{2+} and Mg^{2+} ions were successfully detected by this method (Table 4).

Table 4 Indirect amperometric detection of non-electroactive species at ZMEs

Analyte	Zeolite	Method	References
Li^+, Na^+, Cs^+, Rb^+, Ca^{2+}, Mg^{2+}	Zeolites Y, A, or X exchanged with Cu or Ag	CPE	[57]
NH_4^+	Clinoptilolite	CPE	[58]
K^+	Cu-exchanged A, X, Y zeolites	CPE	[12,59]

Amperometric biosensors

Zeolites can be used in enzyme-containing CPEs with respect to the construction of first-generation biosensors [5]. Due to zeolites hydrophilicity, the exposition of the enzyme contained in the carbon paste to the substrate solution is improved. On the other hand, non-size-excluded cationic mediators can be incorporated in the three-dimensional architecture of zeolites to serve as efficient electron shuttles between the enzyme and the electrode surface.

Some examples of biosensors containing zeolites as immobilization matrices for different enzymes are presented in Table 5.

Table 5 Amperometric biosensors based on ZMEs.

Analyte	Zeolite	Enzyme	Method	Reference
Glucose	NaY + Rh–C particles	GOx	CPE	[60]
Glucose	Y zeolite + PVA	GOx	Deposition/Pt	[61]
H_2O_2	NaY + MG + polystyrene	HRP	Deposition onto GC	[62]
H_2O_2	β-type zeolite + MB + polystyrene	HRP	Deposition onto GC	[63]
Urea	Clinoptilolite membrane	Urease	Immobilization on ammonium-sensitive field-effect transistor	[64]
Phenol	Gelatin/zeolite/G	HRP	Pellets	[46,65]

Potentiometric detection with zeolitic membranes

The ion-exchange properties of zeolites were exploited for preparing ion-selective membranes for potentiometric sensing. Such membranes were prepared for alkaline cations and for some divalent species or drug detection [66–68].

Zeolite-modified carbon paste electrodes (Z-CPEs)

One of the most flexible ways to obtain chemically modified electrodes with zeolites is their incorporation in carbon paste. Mixtures made of spectroscopic graphite powders (as a carbon moiety) and of either paraffin, mineral oils, or silicone fluids were employed in the bare configuration or as chemically modified CPEs, for different analytical purposes [16,69].

In general, CPEs are popular because they are easily obtainable at minimal costs and are especially suitable for preparing an electrode material modified with admixtures of various compounds that give the electrode certain pre-determined properties. Other advantages of CPEs are low background current, wide potential window, and versatility.

Z-CPEs keep all these advantages, and, in addition, the use of zeolites allows the immobilization of large amounts of efficient mediators, such as redox dyes, with significant solubility in specific experimental conditions. Moreover, incorporation of hydrophilic zeolites in carbon paste offers a better exposition of enzymes to the substrate solution in the case of biosensors based on ZMEs. Some examples of new Z-CPEs prepared in our laboratory for amperometric detection of several analytes of practical interest are presented below.

Modified Z-CPEs for amperometric detection of NADH

ZMEs based on carbon paste incorporating soluble redox mediators adsorbed on X-type zeolites were prepared and characterized in our laboratory, aiming to use them for amperometric detection of NADH. Due to its participation in the enzymatic catalysis of more than 300 dehydrogenases, useful both in bioprocesses and in analytical applications, considerable effort has been devoted all over the world to the goal of identifying new electrode materials or mediators to allow the stable determination of NADH at low overpotentials [70].

In this context, two strategies were used for ZME preparation:

(i) Incorporation of NaX zeolites, previously modified with a phenothiazine dye (methylene blue, MB, or methylene green, MG), in carbon paste.

MB and MG are water-soluble cationic phenothiazine dyes with high affinity for zeolitic surfaces. Due to their redox properties, and to their formal potentials very close to most of the biomolecules redox potential, the modified electrodes based on MB and MG as electron mediator system may be of great interest in electroanalytical chemistry. However, the introduction of these mediators directly in the carbon paste does not provide stable sensing devices, due to the leaching process which takes place. To

overcome this problem, zeolites can be used as immobilization matrices, because the channels and the cavities of a zeolite framework offer ideal space for incorporation, stabilization, and organization of the redox mediator. Hence, the zeolitic matrix protects the dye from the surrounding environment and provides signal enhancement due to an increase in the number of dye molecules per nanoparticle.

(ii) Incorporation of an X-type calcium-exchanged zeolite modified with MB in carbon paste.

Knowing that Ca^{2+} cations function as promoters for NADH oxidation in solution [71–75], our main goal was to verify if they also have a beneficial effect when they are immobilized in the zeolite.

For these purposes, an X-type, mesoporous zeolite (13X Aldrich, $1Na_2O{:}1Al_2O_3{:}2.8 \pm 0.2\ SiO_2 \times H_2O$; particle size, 3–5 μm; pore diameter, 10 Å; specific surface area, 548.69 m^2/g; bulk density 480.55 kg/m^3, Si/Al ratio 1.5) was used both in Na and Ca form. Zeolite modification with calcium was realized in a batch reactor in coupled stirring and static conditions. The calculated Ca^{2+} quantity retained on the zeolite was 1.81 mg Ca^{2+}/g zeolite.

The zeolites were modified with MB or MG by adsorption from aqueous solutions during 3 days, under continuous stirring. The modified zeolite was filtered, washed, and dried, then was mixed with graphite powder and paraffin oil and put into a cylindrical holder in order to obtain the modified CPEs.

The presence of adsorbed MB on 13X zeolite was detected with evidence by energy-dispersive spectrometry (EDS) measurements, which indicate the presence of N, S, and Cl belonging to MB. As can be observed from the scanning electron microscopy (SEM) micrographs, the modification of zeolite with MB also determines an agglomeration of zeolite particles (Fig. 2) [18].

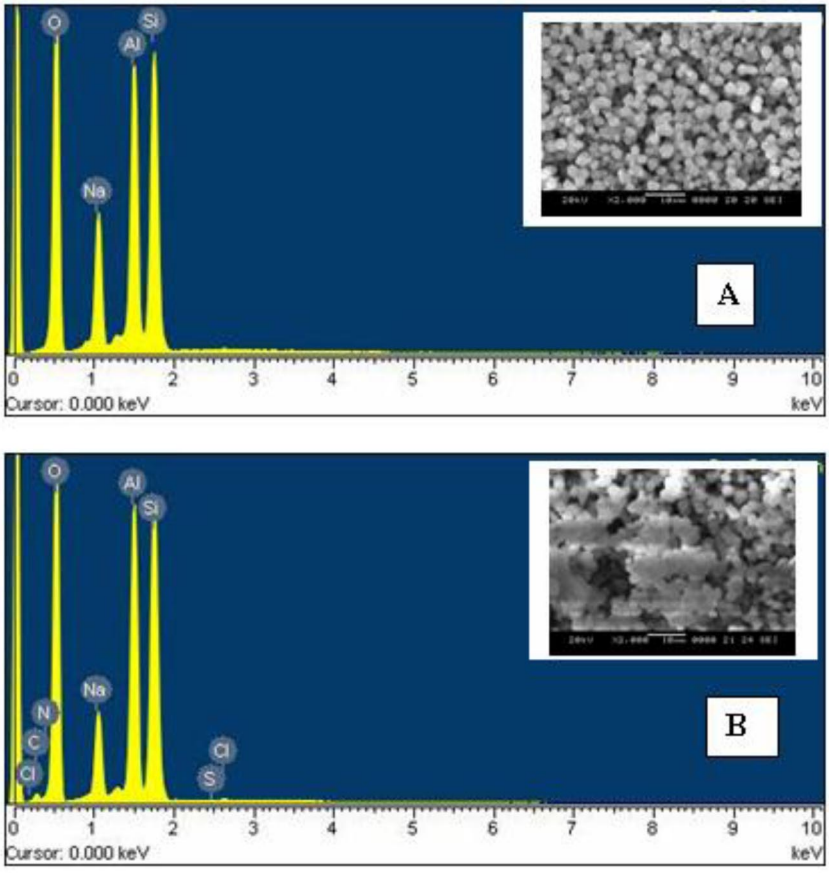

Fig. 2 EDS spectra and SEM images (inset) for 13X zeolite (A) and 13X zeolite modified with MB (B).

Cyclic voltammetric experiments carried out using CPEs containing 13X and 13XCa zeolites modified with MB (MB-13X-CPEs and MB-13XCa-CPEs, respectively) provided evidence of a pair of well-defined redox waves (Fig. 3) [19] that were assigned to the oxidation/reduction of MB adsorbed on the 13X and 13XCa zeolites.

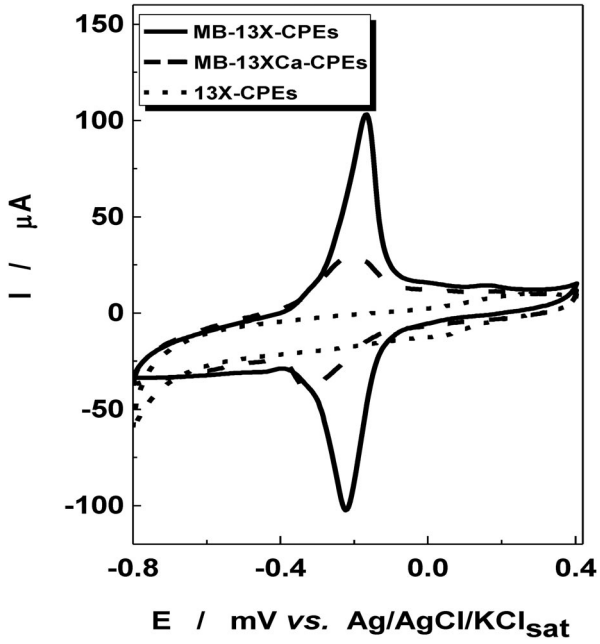

Fig. 3 Cyclic voltammograms for 13X-CPEs (····), MB-13X-CPEs (——) and MB-13XCa-CPEs (– –) electrodes. Experimental conditions: starting potential, –800 mV vs. Ag/AgCl/KCl_{sat}; potential scan rate, 10 mV s^{-1}; supporting electrolyte, 0.1 M phosphate buffer, pH 7.

The peak separation ΔE_p ($\Delta E_p = E_{pa} - E_{pc}$) indicates a quasi-reversible redox process in both cases (Table 6). However, the peak-to-peak separation increases, and the formal standard potential of the peak pair ($E^{0'}$) is shifted toward a negative direction in the presence of Ca^{2+} in zeolite. Even if the I_{pa}/I_{pc} ratio is close to 1 and almost the same for both electrodes, this shift suggests that the process is less reversible in the case of Ca-modified zeolite. In the same time, the surface coverage with MB decreased 2.5 times in the presence of calcium in zeolite.

Table 6 Electrochemical parameters of carbon paste incorporating 13X and 13XCa zeolites modified with MB.

Electrode	E_{pa} V vs. Ag/AgCl	E_{pc} V vs. Ag/AgCl	$E^{0'}$ V vs. Ag/AgCl	ΔE_p V	I_{pa}/I_{pc}	Γ nmol cm^{-2}
MB-13X-CPE	–0.170	–0.223	–0.197	0.053	1.2	88
MB-13XCa-CPE	–0.215	–0.322	–0.269	0.107	1.3	34

Using the treatment proposed by Laviron [77], from the variation of the peak potentials (E_p) with the potential scan rate (v), (eq. 1), the heterogeneous electron-transfer rate constant (k_s, s^{-1}) was estimated (Fig. 4).

$$E_p - E^{0'} = \frac{2.3RT}{\alpha nF} \cdot \lg \frac{\alpha nF}{RTk_s} + \frac{2.3RT}{\alpha nF} \lg v \quad (1)$$

The determined k_s values are evidence of a slower charge transfer in the case of ZMEs prepared with Ca-exchanged zeolite (k_s = 5.5 s^{-1} for MB-13X-CPE and 1.2 s^{-1} for MB-13Ca-CPE at pH 7) [19]. It is supposed that the MB-oxidized form forms a complex with Ca^{2+} and, consequently, the kinetic of electron transfer on the MB-13XCa-CPEs surface is slowed down.

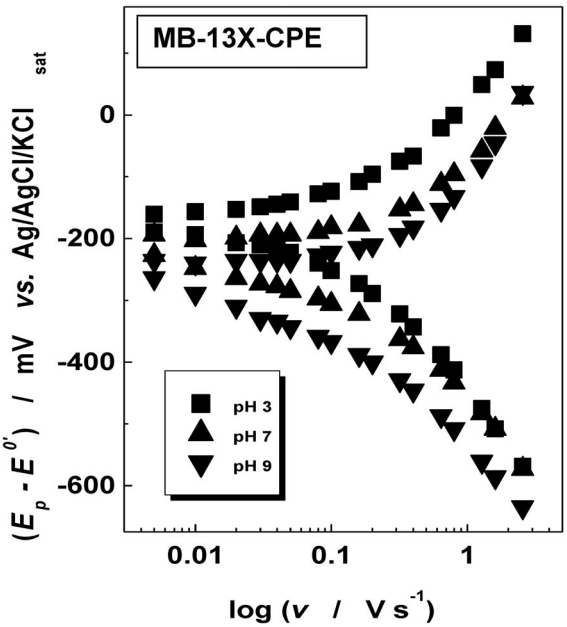

Fig. 4 Experimental dependence of ($E_p - E^{0'}$) on the logarithm of potential scan rate for MB-13X-CPEs, at different pH. Experimental conditions: starting potential, –800 mV vs. $Ag/AgCl/KCl_{sat}$; potential scan rate, 10 mV s^{-1}; supporting electrolyte, 0.1 M phosphate buffer.

The heterogeneous electron-transfer rate constant is not significantly affected by the pH of supporting electrolyte, remaining close to 5 s^{-1} (Table 7) [18]. These results show that MB immobilized on the zeolite acts as a good electron mediator, even if the variation of the transfer coefficient (α) value indicates that the redox processes are not fully reversible at all investigated pH values.

Table 7 pH dependence of heterogeneous charge transfer rate constant, k_s, and on the transfer coefficient, α, for MB-13X-CPEs. Experimental conditions: supporting electrolyte, phosphate buffer, pH 7.

pH	k_s (s^{-1})	α	R/no. of exp. points	
			Oxidation	Reduction
3	5.6	0.55	0.998/5	0.999/5
5	5.4	0.61	0.998/5	0.998/6
5	5.5	0.69	0.992/5	0.993/6
7	5.5	0.72	0.996/5	0.999/5
9	4.9	0.79	0.989/5	0.999/5

Another aspect that should be emphasized is the correlation between the peak current and the potential scan rates. The slope of the log I vs. log v dependence is close to unity in the whole studied pH range (3–9), suggesting the existence of a surface-confined redox couple [18]. Taking into account that the molecular size of MB^+ based on van der Waals radii (7.0×16 Å) is close to that of pore diameter of 13X-type zeolite, it is supposed that the dye molecule fits tightly into the zeolite holes and thus does not leach from the electrode surface.

This conclusion is supported also by the results obtained during the study of pH influence on the electrochemical response of MB-13X-CPEs and MB-13XCa-CPEs (Fig. 5).

In the case of MB-13X-CPEs, the slope of $E^{0'}$-pH dependency is very small (5 mV/ΔpH), in spite to the fact that in solution phase, MB behavior is pH-dependent [77]. These results may suggest that MB (guest molecule) is entrapped in the holes of the 13X-type zeolite (host matrix) and is strongly held by electrostatic interactions, probably involving the amino groups of MB at positions 3 and 7, as well as the heterocyclic nitrogen. The adsorption of MB into the channels of the synthetic zeolite takes place in a confined position and, consequently, it is not affected by the external solution pH change.

A similar behavior was also observed when MB was adsorbed on another zeolite (4A Aldrich, particle size, 2–3 μm; pore diameter, 4 Å; bulk density 480.55 kg/m^3; Si/Al ratio 1, Fig. 5B) and when MG was adsorbed on a NaX-type synthetic zeolite (Bayer, pore size 4.3 Å; Si/Al ratio 1.5, Fig. 5C). The almost constant value for $E^{0'}$ when using MB or MG adsorbed on the above-mentioned zeolites is the basis to recommend the corresponding modified CPEs for obtaining chemical sensors for real samples, where the pH plays an important role and cannot be changed in order to optimize the electrode response.

In contrast, for MB-13XCa-CPEs, $E^{0'}$ varies with the pH. A reasonable explanation for this behavior has not been found yet.

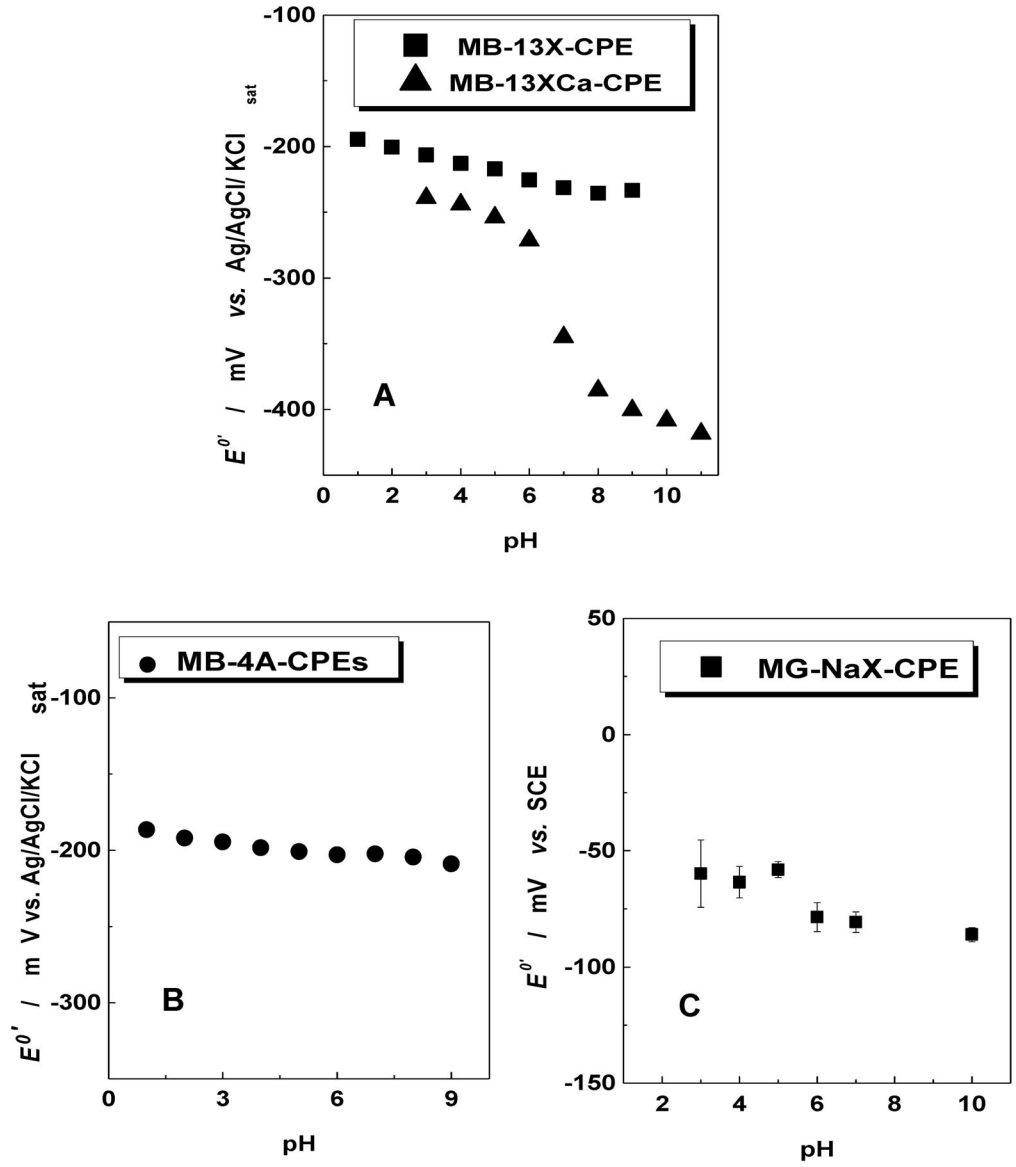

Fig. 5 Variation of $E^{0'}$ with pH for CPEs containing different zeolites modified with MB (**A,B**) or MG (**C**). Experimental conditions: supporting electrolyte, 0.1 M phosphate buffer; potential scan rate 10 mV s^{-1}.

Knowing the beneficial effect of calcium ions on NADH oxidation, comparative cyclic voltammetric measurements were performed for MB-13X-CPEs and MB-13XCa-CPEs in the absence and presence of NADH (Fig. 6) [19]. In both cases, an increase of the anodic current was noticed, the effect being stronger in the presence of Ca-modified zeolite, pointing to an electrocatalytic activity of the electrodes.

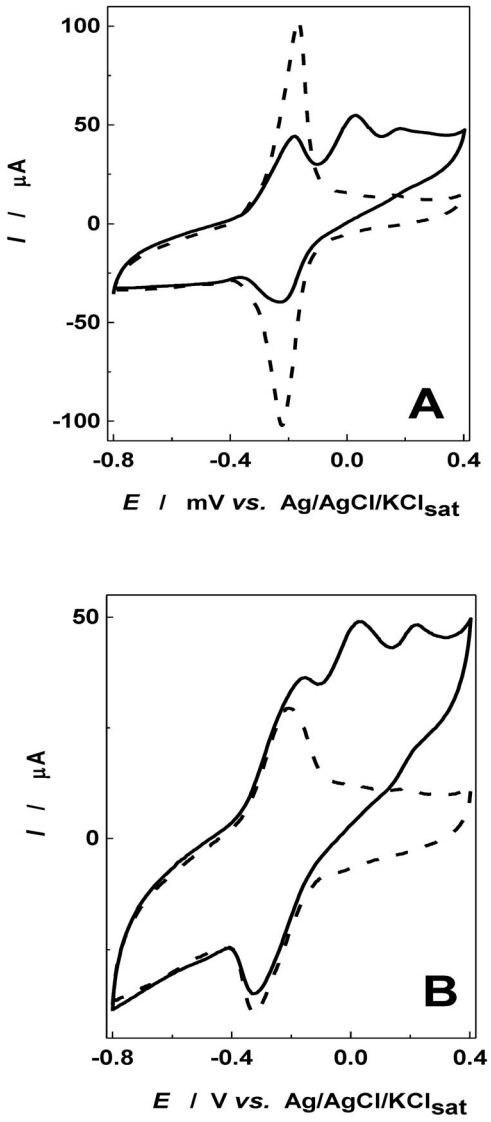

Fig. 6 Cyclic voltammograms obtained at MB-13X-CPEs (A) and MB-13XCa-CPEs (B), in the absence (– –) and in the presence of 10 mM NADH (——). Experimental conditions: starting potential, –800 mV vs. $Ag/AgCl/KCl_{sat}$; potential scan rate, 10 mV s^{-1}; supporting electrolyte, 0.1 M phosphate buffer, pH 7.

One possible explanation of this effect is that Ca^{2+} acts as a bridging ion between NADH and the mediator through the nitrogen atom, coordinating their interaction and thus enhancing the electron-transfer efficiency. Another explanation could be the complexation of Ca^{2+} with the two phosphate groups of NADH, increasing its hydrophobicity, and thus, its affinity toward the hydrophobic molecules of the charge-transfer mediator.

To confirm the effect of calcium cations on the reaction kinetics, we tried to estimate the electrocatalytic rate constant by rotating disk electrode experiments. From Koutecky–Levich plot of I^{-1} vs. $\omega^{-1/2}$ for different NADH concentrations (eq. 2 and Fig. 7), the electrocatalytic rate constant (k_{obs}) was estimated.

$$\frac{1}{I} = \underbrace{\frac{1}{nFAk_{obs}\Gamma[\mathrm{NADH}]}}_{A} + \underbrace{\frac{1}{0.62nFAv^{-1/6}D^{2/3}[\mathrm{NADH}]}}_{B} \cdot \frac{1}{\omega^{1/2}} \quad (2)$$

In eq. 2, n stands for the transferred electrons number; F, for Faraday's constant (96 500 C); $k_{obs,}$ for the electrocatalytic rate constant; Γ, for the surface coverage with mediator molecules; A, for the surface area of the electrode; v, for the viscosity coefficient; D, for the diffusion coefficient; and ω, for the rotation speed of the rotating disc electrode.

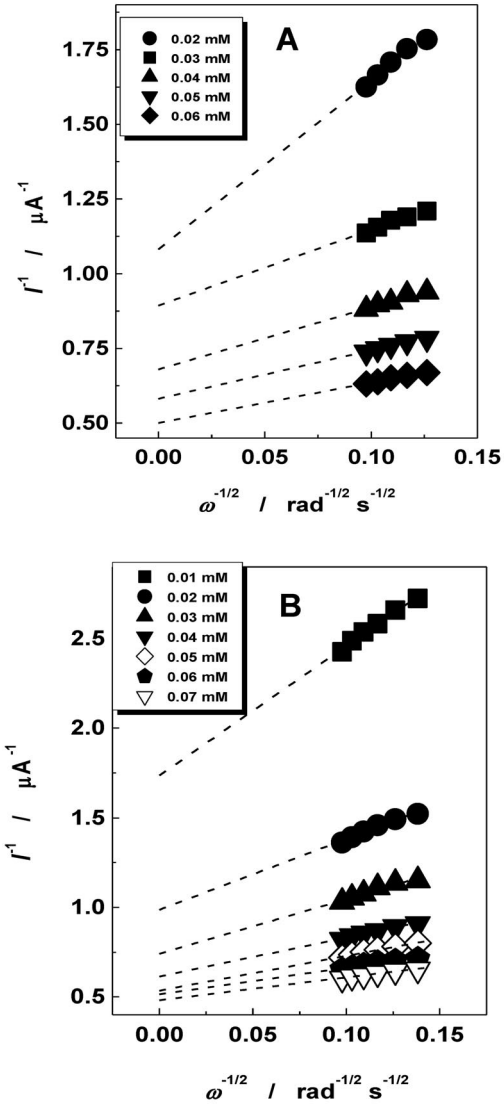

Fig. 7 Koutecky–Levich plots for different concentrations of NADH at MB-13X-CPE (**A**) and MB-13XCa-CPE modified electrodes (**B**); Experimental conditions: supporting electrolyte, phosphate buffer (pH 7); applied potential, 0 mV vs. $Ag/AgCl/KCl_{sat}$.

The dependences of k_{obs} on the NADH concentration were linearized in the coordinates k_{obs}^{-1} vs. [NADH] and $k_{obs,[NADH]=0}$ were calculated by extrapolating the plots to [NADH] = 0. An enhancement of the reaction rate by a factor of 20 was observed in the case of Ca-modified zeolite electrode ($k_{obs,[NADH]=0}$ = 35.5 M^{-1} s^{-1} for MB-13X-CPEs and 704.2 M^{-1} s^{-1} for MB-13XCa-CPEs). A possible explanation is the fact that the [NADH···Ca^{2+}···MB] complex initially formed has a much higher affinity toward NADH than MB itself. Probably Ca^{2+} cations, functioning as promoters for NADH oxidation, provide a favorable orientation of the NADH molecules for this redox process.

Amperometric measurements were performed at constant applied potential (0 mV vs. $Ag/AgCl/KCl_{sat}$) to study the influence of NADH concentration on the electrocatalytic current. A direct consequence of the positive effect of calcium cations on the process kinetics is an increase of the linear range of the calibration curve (Fig. 8A). Moreover, the sensitivity increased from 0.012 to 0.031 A M^{-1} by including Ca^{2+} in the zeolite framework, and the detection limits decreased from 4.3 μM for MB-13X-CPEs to 0.8 μM for MB-13XCa-CPEs.

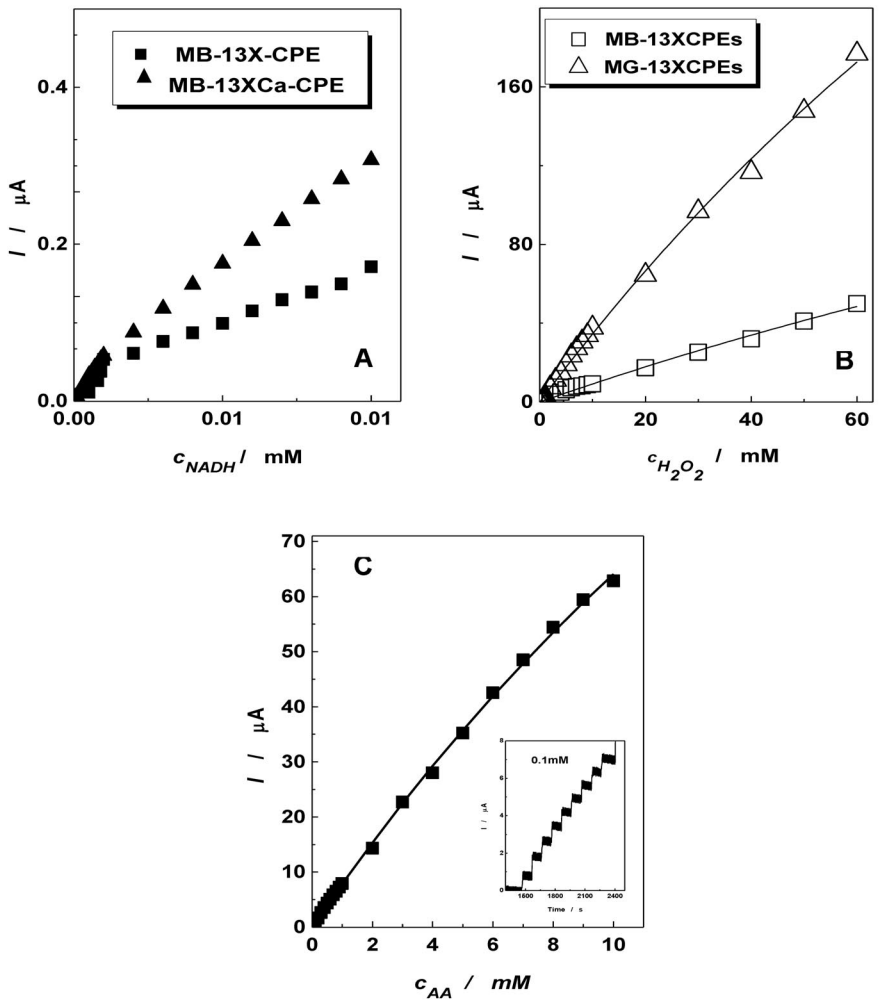

Fig. 8 Calibration curves at MB-13X-CPEs (**A, B, C**) and MG-Z-CPE (**B**) modified electrodes based on the amperometric response to successive increments of NADH (**A**); H_2O_2 (**B**) and AA (**C**). Experimental conditions: applied potential, 0 mV vs. $Ag/AgCl/KCl_{sat}$ (**A**); –0.4 V vs. $Ag/AgCl/KCl_{sat}$ (**B, C**); rotation speed, 1000 rpm; supporting electrolyte, 0.1 M phosphate buffer, pH 7.

The conclusion that can be drawn is that Ca^{2+} ions exert a beneficial effect on NADH oxidation not only in solution, but also when they are immobilized in the zeolite framework. This fact could be exploited successfully to prepare efficient zeolite-based electrode materials for NADH detection.

Modified Z-CPEs for amperometric detection of H_2O_2

A second application of the CPEs modified with MB and MG immobilized on 13X zeolite was for H_2O_2 detection [18].

Based on the favorable electrochemical behavior of MB-13X-CPEs and MG-13X-CPEs, the electrocatalytic activity of the two modified electrodes toward H_2O_2 electroreduction process was investigated by using cyclic voltammetry. An enhancement of the voltammetric cathodic currents in the case of both electrodes immersed in H_2O_2 solutions of different concentrations, and a small peak potential shift toward negative direction when increasing the H_2O_2 concentration, were noticed (results not shown). This voltammetric response indicated that both electrodes exhibited electrocatalytic activity in the above-mentioned process.

Batch amperometric measurements at constant applied potential proved that both MB-13X-CPEs and MG-13X-CPEs work well as amperometric sensors for H_2O_2. The dependence of the catalytic current intensities on H_2O_2 concentrations was shown to be linear (Fig. 8B).

A comparison between the electroanalytical parameters of CPEs containing MB and MG adsorbed on the same zeolite (Table 8) led to the conclusion that MG-13X-CPEs present a better sensitivity and electrocatalytic efficiency than MB-13X-CPEs. Hence, a small difference in the molecular structure of the mediator can result in variations of the electroanalytical parameters of the corresponding modified electrodes. In this case, the presence of acceptor group $–NO_2$ in the structure of MG enhanced the electrocatalytic efficiency [78].

Table 8 Analytical parameters corresponding to MB-13X-CPE and MG-13X-CPE electrodes as amperometric sensors for H_2O_2.

Electrode	Mediator	pH	Detection limit (mM)	Linear domain (M)	Sensitivity (mA/M)		R/N
					M–M*	Slope	
MB-13X-CPEs	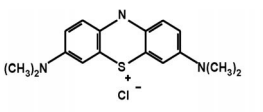	6	0.13	$10^{-4} – 3 \times 10^{-1}$	0.94	1.20	0.991/8
		7	0.79	$8 \times 10^{-4} – 10^{-1}$	1.77	1.80	0.986/15
MG-13X-CPEs	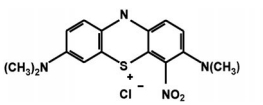	6	0.42	$4 \times 10^{-4} – 2 \times 10^{-1}$	3.63	3.90	0.999/17
		7	0.60	$6 \times 10^{-4} – 1$	2.02	2.00	0.995/20

*Determined by fitting with Michaelis–Menten equation.

The good electrocatalytic efficiency, resulting in relatively low detection limits and large linear response range, can be a recommendation for MB-13X-CPE- and MG-13X-CPE-modified electrodes as transducers for amperometric biosensors based on H_2O_2 detection.

Modified Z-CPEs for amperometric detection of ascorbic acid

Another interesting application of MB-13X-CPEs is the electro-oxidation of ascorbic acid (AA), also known as vitamin C, an organic compound that plays an important role in living bodies. L-Ascorbic acid is widely used as a dietary supplement and is also added to manufacture foods as an antioxidant for preservation [79]. Consequently, measuring AA content is very important for assessing food product quality.

The electrocatalytic activity of MB-13X-CPEs was investigated by using cyclic voltammetry measurements (results not shown), in the absence and presence of AA (phosphate buffer, pH 7). An enhancement of the anodic current in the presence of AA at significantly lower potentials than those registered on unmodified CPEs [80] was observed, proving the electrocatalytic effect. The calibration curves, based on the amperometric response of MB-13X-CPEs to successive injections of 0.1 mM AA (applied potential –50 mV vs. $Ag/AgCl/KCl_{sat}$) (Fig. 8C), present a linear domain from 10^{-5} to 10^{-3} M AA [81]. The theoretical detection limits, calculated from the slope of the regression equation and standard deviation of the calibration curves (4.7×10^{-5} M), the good sensitivity (8×10^{-3} A/M) and the relatively short time response (5 s), suggest that MB-13X-CPEs can be used as amperometric sensors for AA.

CONCLUSIONS

Based on the above-mentioned experimental results, some conclusions have been drawn:

- Zeolites represent a successful solution for immobilizing soluble redox dyes, in order to obtain stable electrode materials exhibiting good catalytic activity toward oxidation/reduction of different chemical species of practical interest
- Zeolites modified with MB or MG incorporated in carbon paste are promising materials for obtaining chemical sensors to be used in solutions where the pH varies or cannot be changed in order to optimize the electrode response.
- Ca^{2+} cations function as promoters for NADH oxidation not only in solution, but also when they are immobilized in the zeolite framework. The electroanalytical parameters of the ZMEs are sensibly improved in the case when CaX zeolite was used for the electrode preparation, as compared to the case when the same zeolite is used in Na form.

ACKNOWLEDGMENTS

Financial support from the National Council for Scientific Research in Higher Education of Romania (CNCSIS, Grant PN II 71-098/18.09.2007) is gratefully acknowledged. The author thanks Ph.D. student C. Varodi, Associate Prof. D. Gligor and Associate Prof. A. Maicaneanu for their contribution.

REFERENCES

1. D. R. Rolison. *Chem. Rev.* **90**, 867 (1990).
2. A. Walcarius. *Electroanalysis* **8**, 971 (1996).
3. Ch. Baerlocher, W. M. Meyer, D. H. Olson. *Atlas of Zeolites Framework Types*, 5th revised ed., Elsevier, London (2001).
4. W. Shan, Y. Zhang, W. Yang, C. Ke, Z. Gao, Y. Ye, Y. Tang. *Microporous Macroporous Mater.* **69**, 35 (2004).
5. A. Walcarius. *Anal. Chim. Acta* **384**, 1 (1999).
6. D. R. Rolison, R. J. Nowak, T. A. Welsh, C. G. Murray. *Talanta* **38**, 27 (1991).
7. J. Lipkowski, P. Ross. In *The Electrochemistry of Novel Materials*, p. 339, VCH, New York (1994).
8. S. M. Kuznicki, V. A. Bell, T. W. Langner, J. S. Curran. U.S. Patent 6572776, B01J39/14 (2003).
9. S. K. Ouki, M. Kavannagh. *Waste Manage. Res.* **15**, 383 (1997).
10. E. Álvarez-Ayuso, A. García-Sánchez, X. Querol. *Water Res.* **37**, 4855 (2003).
11. D. R. Rolison, C. A. Bessel. *Acc. Chem. Res.* **33**, 737 (2000).
12. M. Granda-Valdes, A. I. Perez-Cordoves, M. E. Diez-Garcia. *Trends Anal. Chem.* **25**, 2430 (2006).

13. S. Kilinc Alpat, U. Yuksel, H. Akcay. *Electrochem. Commun*. **7**, 130 (2005).
14. S. Senthilkumar, R. Saraswathi. *Sens. Actuators, B* **141**, 65 (2009).
15. L. Li, W. Li, C. Sun, L. Li. *Electroanalysis* **14**, 368 (2002).
16. A. Walcarius, P. Mariaulle, L. Lamberts. *J. Solid State Electrochem.* **7**, 671 (2003).
17. A. Walcarius, L. Lamberts, E. G. Derouane. *Electrochim. Acta* **38**, 2257 (1993)
18. C. Varodi, D. Gligor, L. M. Muresan. *Rev. Roum. Chim*. **52**, 81 (2007).
19. C. Varodi, D. Gligor, A. Măicăneanu, L. M. Muresan. *Rev. Chim.* **9**, 890 (2007).
20. D. Gligor, L. M. Muresan, A. Dumitru, I. C. Popescu. *J. Appl. Electrochem*. **37**, 261 (2007).
21. M. B. Berry, B. E. Libby, K. Rose, K.-H. Haas, R. W. Thompson. *Microporous Macroporous Mater*. **39**, 205 (2000).
22. M. P. Vinod, T. Kr. Das, A. J. Chandwadkar, K. Vijayamohanan, J. G. Chandwadkar. *Mater. Chem. Phys.* **58**, 37 (1999).
23. M. D. Baker, C. Senaratne, J. Zhang. *J. Phys. Chem*. **98**, 1668 (1994).
24. M. D. Baker, J. Zhang, M. McBrien. *J. Phys. Chem*. **99**, 6635 (1995).
25. D. H. Brouwer, M. D. Baker. *J. Phys. Chem. B* **101**, 10390 (1997).
26. C. Song, G. Villemure. *Microporous Macroporous Mater.* **44–45**, 679 (2001).
27. F. Bedioui, E. de Boisson, J. Devynck, K. J. Balhus Jr. *J. Electroanal. Chem*. **315**, 313 (1991).
28. C. G. Murray, R. J. Nowak, D. R. Rolison. *J. Electroanal. Chem*. **164**, 205 (1984).
29. P. Enzel, Th. Bein. *J. Chem. Soc., Chem. Commun*. 1326 (1989).
30. G. F. McCann, G. J. Millar, G. A. Bowmaker, R. P. Cooney. *J. Chem. Soc., Faraday Trans*. **91**, 4321 (1995).
31. G. J. Millar, G. F. McCann, C. M. Hobbis, G. A. Bowmaker, R. P. Cooney. *J. Chem. Soc., Faraday Trans*. **90**, 2579 (1994).
32. H. Uehara, M. Miyake, M. Matsuda, M. Sato. *J. Mater. Chem*. **8**, 2133 (1998).
33. T. H. Chao, H. A. Erf. *J. Catal.* **100**, 492 (1986).
34. A. Matsumoto, T. Kitajima, K. Tsutsumi. *Langmuir* **15**, 7626 (1999).
35. A. Domenech, H. Garcia, E. Carbonell. *J. Electroanal. Chem*. **577**, 249 (2005).
36. M. Alvaro, B. Ferrer, H. Garcia, A. Lay, F. Trinidad, J. Valenciano. *Chem. Phys. Lett.* **356**, 577 (2002).
37. Z. Li, C. Lai, T. E. Malouk. *Inorg. Chem*. **28**, 178 (1989).
38. C. B. Ahlers, J. B. Talbot. *Electrochim. Acta* **45**, 3379 (2000).
39. P. K. Dutta, M. Ledney. *Prog. Inorg. Chem*. **44**, 209 (1977).
40. K. E. Creasy, B. R. Shaw. *Electrochim. Acta* **33**, 551 (1988).
41. H. A. Gemborys, B. R. Shaw. *J. Electroanal. Chem.* **208**, 95 (1986).
42. S. V. Guerra, C. R. Xavier, S. Nakagaki, L. T. Kubota. *Electroanalysis* **10**, 462 (1998).
43. V. Ganesan, R. Ramaraj. *J. Appl. Electrochem.* **30**, 757 (2000).
44. S. Serban, N. El Murr. *Biosens. Bioelectron.* **20**, 161 (2004).
45. M. M. Ardakani, Z. Akrami, H. Kazemian, H. R. Zare. *J. Electroanal. Chem*. **586**, 31 (2006).
46. R. H. Carvalho, M. A. N. D. A. Lemos, F. Lemos, J. M. S. Cabral, F. Ramoa Ribeiro. *J. Mol. Catal. A: Chem.* **253**, 170 (2006).
47. D. Bergé-Lefranc, M. Eyraud, O. Schaf. *C. R. Chim.* **11**, 1063 (2008).
48. T. Rohani, M. A. Taher. *Talanta* **78**, 743 (2009).
49. D. Gligor, A. Maicaneanu, A. Walcarius. *Electrochim. Acta* **55**, 4050 (2010).
50. B. R. Shaw, K. E. Creasy. *J. Electroanal. Chem*. **243**, 209 (1988).
51. J. Wang, T. Martinez. *Anal. Chim. Acta* **207**, 95 (1988).
52. J. Wang, A. Walcarius. *J. Electroanal. Chem*. **407**, 183 (1996).
53. M. del Mar Cordero-Rando, M. Barea-Zamora, J. M. Barbera-Salvador, I. Naranjo-Rodriguez, J. A. Munoz-Leyva, J. L. Hidalgo-Hidalgo de Cisneros. *Mikrochim. Acta* **132**, 7 (1999).
54. C. Bing, L. Kryger. *Talanta* **43**, 153 (1996).
55. A. Babaei, M. Zendehdel, B. Khalilzadeh, A. Taheri. *Colloids Surf., B* **66**, 226 (2008).

56. M. Arvand, M. Vaziri, M. Vejdani. *Mater. Sci. Eng. C* **30**, 709 (2010).
57. A. Walcarius, P. Mariaulle, C. Louis, L. Lamberts. *Electroanalysis* **11**, 393 (1999).
58. A. Walcarius, V. Vromman, J. Bessière. *Sens. Actuators, B* **56**, 136 (1999).
59. A. Walcarius. *Anal. Chim. Acta* **388**, 79 (1999).
60. J. Wang, A. Walcarius. *J. Electroanal. Chem.* **404**, 237 (1996).
61. B. Liu, R. Hiu, J. Deng. *Anal. Chem.* **69**, 2343 (1997).
62. B. Liu, F. Yan, J. Kong, J. Deng. *Anal. Chim. Acta* **386**, 31 (1999).
63. B. Liu, Z. Liu, D. Chen, J. Kong, J. Deng. *Fresenius' J. Anal. Chem.* **367**, 539 (2000).
64. M. L. Hamlaoui, K. Reybier, M. Marrakchi, N. Jaffrezic-Renault, C. Martelet, R. Kherrat, A. Walcarius. *Anal. Chim. Acta* **466**, 39 (2002).
65. R. H. Carvalho, F. Lemos, M. A. N. D. A. Lemos, J. M. S. Cabral, F. Ramoa Ribeiro. *J. Mol. Catal. A: Chem*. **278**, 47 (2007).
66. A. N. Ejhieh, N. Masoudipour. *Anal. Chim. Acta* **658**, 68 (2010).
67. B. Vissers, H. Bohets, J. Everaert, P. Cool, E. F. Vansant, F. Du Prez, J. M. Kauffmann, L. J. Nagels. *Electrochim. Acta* **51**, 5062 (2006).
68. M. Arvand-Barmchi, M. F. Mousavi, M. A. Zanjanchi, M. Shamsipur. *Sens. Actuators, B* **96**, 560 (2003).
69. I. Švancara, A. Walcarius, K. Kalcher, K. Vytřas. *Cent. Eur. J. Chem*. **7**, 598 (2009).
70. L. Gorton, E. Dominguez. *Encyclopedia of Electrochemistry*, **9**, G. S. Wilson (Ed.), Wiley-VCH, New York (2002).
71. E. Katz, T. Lötzbeyer, D. D. Schlereth, W. Schuhmann. *J. Electroanal. Chem*. **373**, 189 (1994).
72. N. Mano, A. Kuhn. *Electrochem. Commun*. **498**, 58 (2001).
73. N. Mano, A. Kuhn. *Electrochem. Commun*. **1**, 497 (1999).
74. C.-S. Toh, P. N. Bartlett, N. Mano, F. Aussenac, A. Kuhn, E. J. Dufourc. *Phys. Chem. Chem. Phys.* **5**, 588 (2003).
75. N. Mano, A. Kuhn, S. Menu, E. J. Dufourc. *Phys. Chem. Chem. Phys*. **5**, 2082 (2003).
76. E. Laviron. *J. Electroanal. Chem*. **101**, 19 (1979).
77. S. L. P. Dias, S. T. Fujiwara, Y. Gushikem, R. E. Bruns. *J. Electroanal. Chem*. **292**, 115 (1990).
78. C. Varodi, D. Gligor, L. Abodi, L. M. Muresan. *Studia Univ. Babes-Bolyai, Chemia*, LIV, **3**, 255 (2009).
79. J. C. Bauernfeind, D. M. Pinkert. *Ascorbic Acid as an Added Nutrient to Beverage*, p. 24, Hoffmann-La Roche, Basel (1970).
80. Y. Dilgin, Z. Dursun, G. Nisli, L. Gorton. *Anal. Chim. Acta* **542**, 162 (2005).
81. C. Varodi, D. Gligor, L. M. Muresan. *Studia Univ. Babes-Bolyai, Chemia*, LII, **1**, 109 (2007).

